Acta Scientiarum

http://www.uem.br/acta
ISSN printed: 1806-2563
ISSN on-line: 1807-8664
Doi: 10.4025/actascitechnol.v38i4.27992

Inverse problem for porosity estimation during solidification of TNT

Aldélio Bueno Caldeira[1*], Bruno dos Reis Jaccoud[1,2] and Rodrigo Otávio de Castro Guedes[1]

*[1]Programa de Engenharia Mecânica, Instituto Militar de Engenharia, Praça General Tibúrcio, 80, 22290-270, Rio de Janeiro, Rio de Janeiro, Brazil. [2]Programa de Engenharia de Nanotecnologia, Universidade Federal do Rio de Janeiro, Rio de Janeiro, Brazil. *Author for correspondence. E-mail: aldelio@ime.eb.br*

ABSTRACT. In the present study, the porosity formed during the solidification process is estimated by an inverse problem technique based on particle swarm optimization. The effective heat capacity method is adopted to model the heat transfer problem. The transient-diffusive heat transfer equation is solved numerically by the finite volume method with an explicit scheme, employing the central difference interpolation function. The solution of the direct problem is compared to reference solutions. The model is applied to trinitrotoluene (TNT) solidification process. The results show that the proposed procedure was able to estimate the porosity for different Stefan numbers. The analysis of the heat flux in the mold is indicated to predict the porosity formation during the casting process.

Keywords: solidification, porosity, inverse problem, particle swarm.

Problema inverso de estimativa da porosidade formada durante a solidificação de TNT

RESUMO. No presente trabalho, a formação de porosidade durante o processo de solidificação é estimada por uma técnica de problema inverso baseada na otimização por enxame de partículas. O método da capacidade efetiva de calor é adotado para representar o problema de transferência de calor. A equação transiente-difusiva de transferência de calor é resolvida numericamente pelo método dos volumes finitos com um esquema explícito, empregando a função de interpolação de diferença central. A solução do problema direto é comparada a soluções de referência. O modelo é aplicado ao processo de solidificação do trinitrotolueno (TNT). Os resultados mostram que o procedimento proposto foi capaz de estimar a porosidade para diferentes números de Stefan. A análise do fluxo de calor no molde é indicada para prever a formação de porosidade durante o processo de fundição.

Palavras-chave: solidificação, porosidade, problema inverso, enxame de partículas.

Introduction

The solidification phenomenon is present in nature and in industrial processes. In nature, it can be observed during the formation of ice as well as volcanic lava, while in industry, it is found in freezing, casting and welding (Tan, Li, & Li, 2011, Verma & Gómez-Arias, 2013, Yajun, Pengfei, Yongjun, Zhijun, & Yintao, 2013, Humphreys et al., 2013).

The Stefan problem is the classical mathematical model for the solidification process. It is based on the heat equation in a solid region where the phase change interface is regarded as a moving boundary (Stefan, 1891).

The method of effective heat capacity has been proposed to avoid the difficulties of the Stefan approach in complex geometries. In this method, the solid and liquid regions are solved in a single domain and an effective heat capacity takes into account the phase change phenomenon, considering the existence of a mushy region, where liquid and solid are present (Hu & Argyropoulos, 1996, Poirier & Salcudean, 1998, Mosaffa, Ferreira, Talati, & Rosen, 2013).

The porosity formed during the solidification process should be avoided since it is usually considered a manufacturing defect. Porosity changes the mechanical and thermophysical properties of the material (Zhang, Kim, & Lu, 2009).

The solidification process of casting explosives in artillery shells is used to produce high-explosive ammunitions (HE ammunitions). These ammunitions are filled with explosives that detonate to produce the terminal effect. The presence of pores in the explosive inside these devices is a dangerous problem, since this defect could lead to an undesirable initiation of the explosive in addition to changing the terminal effect, therefore reducing the efficiency of the ammunition (Zhang, Hu, & Liang, 2013, Kumar & Rao, 2014).

The Particle Swarm Optimization (PSO) is based on social behavior of various species and aims at balancing individuality and sociability, in order to optimize a group of parameters. This stochastic and

evolutionary method has been employed in inverse problems for parameters estimation (Colaço, Orlande, & Dulikravich, 2006).

The present study deals with the estimation of porosity formed during the solidification process. A mathematical model with a numerical solution is provided for the direct problem. PSO is used to solve the inverse problem. Trinitrotoluene (TNT) solidification is studied because TNT casting process is often employed in HE ammunitions. Moreover, in such devices, the presence of pores is dangerous and must be avoided.

Material and methods

In this study, a one-dimensional transient heat solidification problem in rectangular coordinates is analyzed. Initially, the entire domain is at uniform temperature and only the liquid phase is present. Suddenly, a temperature lower than the solidification temperature is applied at the origin of the system of coordinates (y = 0) and thus a prescribed temperature is attained at this boundary. Then, the solidification process starts at y = 0 and the solidification front moves away from such boundary. The physical properties of liquid and solid phases are assumed constant at each phase. The effective heat capacity method is adopted (Hu & Argyropoulos, 1996). The mathematical model represented in Equation 1 describes heat transfer in the solid phase, in the liquid phase and in the mushy region.

$$\begin{aligned} &C_{ef}\frac{\partial T}{\partial t}=\frac{\partial}{\partial y}\left(k_{ef}\frac{\partial T}{\partial y}\right), \quad 0<y<L, \quad t>0\\ &T=T_0, \quad 0\le y\le L, \quad t=0\\ &T=T_w, \quad y=0, \quad t>0\\ &\frac{\partial T}{\partial y}=0, \quad y=L, \quad t>0 \end{aligned} \tag{1}$$

In this model, C_{ef} is the effective heat capacity, k_{ef} is the effective thermal conductivity, T is the temperature, t is the time, y is the position, L is the length of the domain, T_0 is the initial temperature and T_w is the wall temperature of the mold.

By applying the Finite Volume Method (FVM) (Maliska, 2004), the effective heat capacity is evaluated at each finite volume as, according Equation 2:

$$C_{ef}=\frac{\int_{T_s}^{T_n} C_{ap}\, dT}{T_n-T_s} \tag{2}$$

The usual nomenclature adopted in FVM is employed in Equation 2. The subscript n is related to the north face of the finite volume, while the subscript s is related to the south face of the finite volume. The apparent heat capacity, C_{ap}, is Equation 3:

$$C_{ap}=\begin{cases} \rho_{solid}\, c_p\,(1-\varepsilon), & T\le T_m-\Delta T\\ \dfrac{\rho_{solid}\,\Delta H}{\Delta T}+ & \\ +0.5\,\rho_{solid}\, c_p\,(1-\varepsilon)+, & T_m-\Delta T<T<T_m+\Delta T\\ +0.5\,\rho_{liquid}\, c_p & \\ \rho_{liquid}\, c_p, & T\ge T_m+\Delta T \end{cases} \tag{3}$$

In Equation 3, ΔH is the latent heat, T_m is the melting temperature and ΔT is half of phase change temperature range, which is a parameter of the effective heat capacity method (Hu & Argyropoulos, 1996). This parameter defines a theoretical mushy region for the evaluation of the effective heat capacity. Furthermore, the subscripts solid and liquid indicate, respectively, the solid phase and the liquid phase. In addition, ρ is the density, c_p is the specific heat and ε is the porosity.

The proposed model considers that the values of thermal conductivity, k, and those of specific heat, c_p, of the TNT are constant and they do not depend on the phase (Sun & Garimella, 2007). Moreover, the specific heat is not a function of the porosity (Gibson & Ashby, 1997). The porosity is the ratio of the volume of the pores to the total volume of the porous medium.

It is common knowledge that porosity changes the thermophysical properties of the solidified region. Therefore, by considering a homogenous distribution for the pores, the effective thermophysical properties must be defined for the porous medium. The pores are also considered spherical in materials with porosity less than 70% (Zhang et al., 2009). In addition, assuming that thermal conductivity is greater in the solid medium than in the pores, the effective thermal conductivity is defined (Bauer, 1993, Wang, Carson, North, & Cleland, 2006, Zhang et al., 2009) as Equation 4:

$$k_{ef}=\begin{cases} k(1-\varepsilon)^{3\beta/2}, & T<T_m\\ k, & T\ge T_m \end{cases} \tag{4}$$

where:

β=1 is used to spherical pores (Zhang et al., 2009).

The buoyancy effects can be neglected in TNT casting (Kumar & Rao, 2014), since TNT viscosity (Sun & Garimella, 2007) is roughly a hundred times

the viscosity of water at 300 K.

In order to solve the problem described by Equation 1, the FVM is employed by using an explicit scheme and the central differences interpolation function (Maliska, 2004). The stability criterion is satisfied and described by Equation 5:

$$\Gamma = \frac{k_{ef}\ \Delta t}{C_{ef}\ \Delta y^2} < 0.5 \tag{5}$$

Simulations were performed in a computer with Quad Core i7-860 (2.80 GHz) processor and 8 Gb RAM, using $\Delta y = 0.0021$ m and $\Delta t = 10$ s, which results in $0.14 \times 10^{-6} \leq \Gamma \leq 0.34$.

The parameters for the model and the physical properties of TNT are presented, respectively, in Table 1 and 2. They are based on real ammunition.

Table 1. Parameters for the model (Jaccoud, Caldeira, & Guedes, 2014).

Parameter	Symbol	Value
Wall temperature	T_w	300 K
Initial temperature	T_0	360 K
Length of the domain	L	0.3419 m
Half of phase change temperature range	ΔT	3.5544 K

Table 2. Thermophysical properties of TNT (Sun & Garimella, 2007, Jaccoud et al., 2014).

Property	Symbol	Value
Density of solid phase	ρ_{solid}	1648 kg m^{-3}
Density of liquid phase	ρ_{liquid}	1544.6 kg m^{-3}
Specific heat	c_o	1062.2 J kg^{-1} K
Thermal conductivity	k	0.26 W m^{-1} K
Melting temperature	T_m	354.05 K
Latent heat	ΔH	98.4 kJ kg^{-1}

The proposed inverse problem estimates the porosity formed during the solidification process of TNT. The inverse problem is an optimization problem, which is solved by using PSO. The optimum solution determines the estimated porosity.

In PSO, each particle i of a given population P in a N dimensional space has a velocity v_i^j and a position x_i^j, which are updated in accordance with Equations 6 and 7:

$$v_i^{j+1} = \omega\ v_i^j + c_1\ r_{1i}\left(p_i - x_i^j\right) + c_2\ r_{2i}\left(p_g - x_i^j\right) \tag{6}$$

$$x_i^{j+1} = x_i^j + v_i^{j+1} \tag{7}$$

where:
i=1, 2,..., P;
j is the iteration of the optimization process;
$v_i^0 = 0$;
r_{1i} and r_{2i} are random numbers between 0 and 1 with uniform distribution;
p_i is the best parameters set of the particle x_i;
p_g is the best parameters set of the population;
ω is the inertial constant within the range [0, 1];
c_1 and c_2 are constants within the range [1, 2].

The PSO is used to estimate the porosity parameter, considering the objective function, according Equation 8:

$$F\left(\varepsilon_i^j\right) = \sum_{z=1}^{nt}\left[S(t_z)_{exp} - S\left(\varepsilon_i^j, t_z\right)_{num}\right]^2 \cong$$
$$\cong k_{ef}\left(T_m - T_w\right)\sum_{z=1}^{nt}\left[q_w^{-1}(t_z)_{exp} - q_w^{-1}\left(\varepsilon_i^j, t_z\right)_{num}\right]^2 \tag{8}$$

where:
S is the position of the solidification front. The subscript $_{exp}$ refers to the experimental data and the subscript $_{num}$ refers to the proposed FVM solution. nt is the total number of evaluated times and q_w is the heat flux at the wall (y = 0), which is expressed as Equation 9:

$$q_w \cong k_{ef}\frac{T_m - T_w}{S} \tag{9}$$

Consequently, Equation 10:

$$S \cong k_{ef}\left(T_m - T_w\right) q_w^{-1} \tag{10}$$

Thus, measurements of the heat flux at the wall (y = 0) (or of the position of the solidification front) could be introduced in the objective function to estimate porosity. However, in the present study, since experimental data were not available, an analytical solution (Zhang et al., 2009) has mimicked the experimental data (Iacono, Sluys, & Van Mier, 2011).

The analytical solution (Zhang et al., 2009) is Equations 11 at 14:

$$\xi = \frac{S}{L} = 2\,\lambda\sqrt{\tau\left(1-\varepsilon\right)^{(3\,\beta/2-1)}} \tag{11}$$

$$\lambda\sqrt{\pi}\exp\left(\lambda^2\right)\mathrm{erf}(\lambda) = \mathrm{Ste} \tag{12}$$

$$\tau = \frac{k\ t}{\rho_{solid}\ c_p\ L^2} \tag{13}$$

$$\mathrm{Ste} = \frac{\rho_{solid}\ c_p\ \left(T_m - T_w\right)}{\Delta H} \tag{14}$$

where:
ξ is the dimensionless position of the solidification front and λ is a theoretical parameter determined from Equation 12, τ is the Fourier number and Ste is the Stefan number.

It is important to note that usually experimental data or synthetic experimental data that could be obtained from a mathematical solution and corrupted by random noise, with a prescribed noise level, are used in inverse problems. Such approach is employed to avoid the inverse crime. However, in this paper, the analytical solution (Zhang et al., 2009) solves the solidification process in a semi-infinite domain, considering a Stefan model, while the numerical solution solves the solidification process in a finite domain, considering the effective heat capacity approach. In this sense, the inverse crime is not present in this study, because the analytical solution is used to simulate experimental data and the numerical solution solves the inverse procedure (Chávez, Alonzo-Atienza, & Álvarez, 2013). However, different levels of random noise were also introduced in the analytical solution (Zhang et al., 2009) by Equation 15:

$$S_{exp} = S_{analytical} + \varpi \, E \, L \quad (15)$$

where:
$S_{analytical}$ is the solidification front computed with the analytical solution (Zhang et al., 2009);
ϖ is a random variable with normal distribution, zero mean and unitary standard deviation;
E is an arbitrary noise level and;
L is the maximum value of $S_{analytical}$ (Machado & Orlande, 1998, Ozisik & Orlande, 2000).

The stopping criterion of the optimization procedure considers that Equation 16 must be satisfied during 50 consecutive iterations.

$$\left| F\left(p_g^{j+1}\right) - F\left(p_g^{j}\right) \right| / F\left(p_g^{j+1}\right) \leq 10^{-8} \quad (16)$$

Results and discussion

Figure 1 and 2 are mainly presented to verify the quality of the proposed numerical solution. Discrepancies between numerical and analytical results for the position of the solidification front are shown when $\xi \rightarrow 1$. They are caused by the finite domain used in the numerical solution and by the semi-infinite domain used in the analytical solution. Such discrepancies are reduced when the length of the finite domain is increased. The influence of the length of the finite domain on the position of the solidification front can be observed in Figure 1, where the results for the solidification of TNT (Ste = 0.58) without pores are presented. By increasing the length of the domain, the numerical solution approaches the analytical solution. Hence, the effective heat capacity method and proposed FVM solution represents correctly the evolution of the solidification front of TNT.

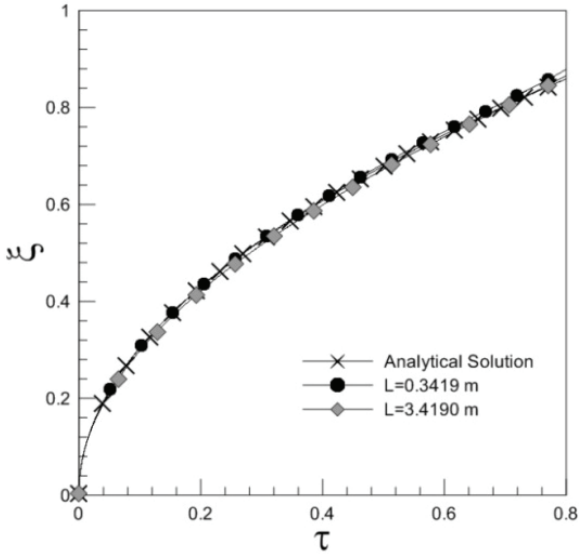

Figure 1. Effects of the domain length on the numerical solution (Ste = 0.58, ε = 0).

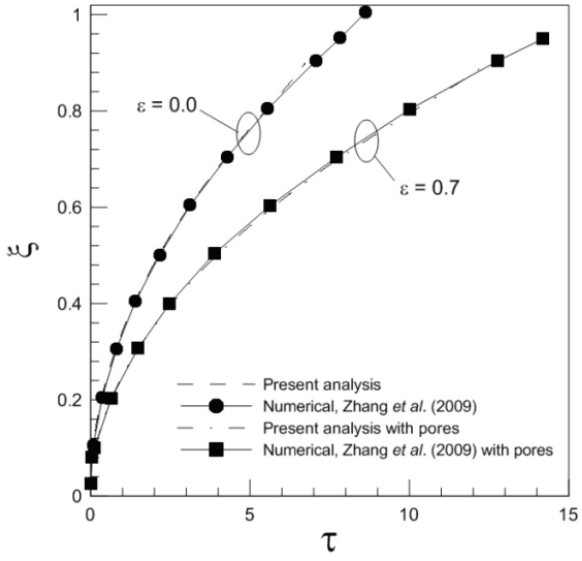

Figure 2. Evolution of the solidification front (Ste = 0.06).

Figure 2 shows the numerical results provided by the present analysis and the ones by Zhang et al. (2009) for the evolution of the solidification front of a metal (Ste = 0.06), considering the cases with pores (ε = 0.7) and without pores (ε = 0.0). The proposed numerical results match the ones by

Zhang et al. (2009). Furthermore, porosity reduces the velocity of the solidification front, since it diminishes the heat transfer. This trend is corroborated by the results shown in Figure 3 for TNT (Ste = 0.58), considering the cases with pores (ε = 0.7) and without pores (ε = 0.0).

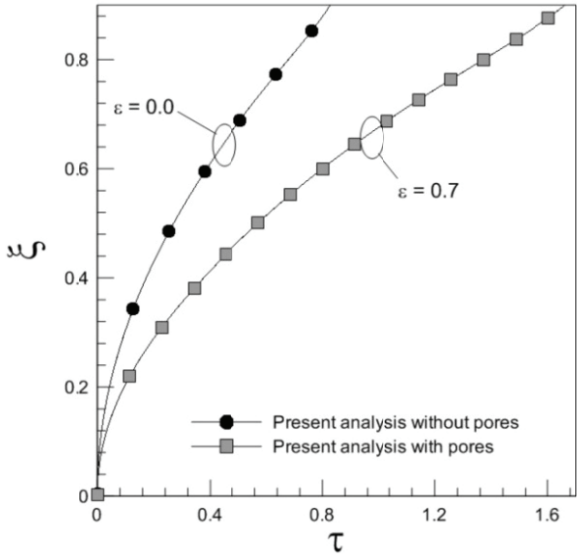

Figure 3. Porosity effects on TNT solidification (Ste = 0.58).

In Figure 4, by increasing the porosity, the displacement of the solidification front is reduced, because the heat transfer in the pores is negligible in relation to the solid material. In other words, the thermal conductivity in the solid is much greater than in the pores. Thus, the presence of pores delays the solidification process.

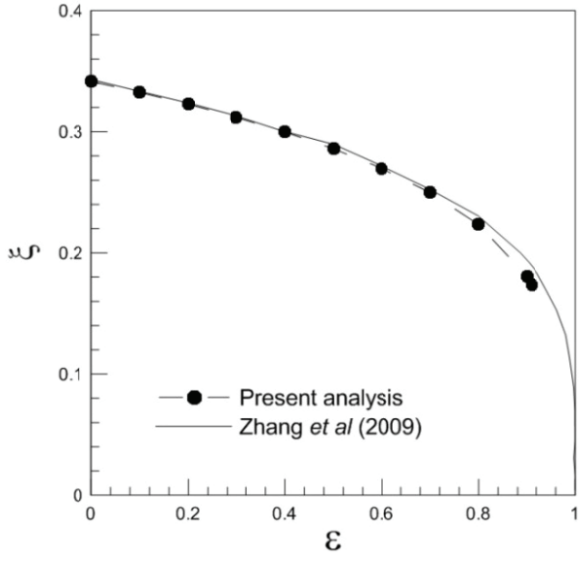

Figure 4. Porosity effects on the solidification front of TNT (Ste = 0.58, τ = 0.5).

Figure 5 reports the evolution of the objective function for populations with different sizes, considering synthetic experimental data for the cases with pores (ε = 0.7) and without pores (ε = 0.0). The number of particles on the inverse problem procedure is not relevant. The values for the objective function attained for each population are very similar. Therefore, a smaller population is recommended to perform simulations, since it demands smaller computation time. The results in Table 3 confirm this statement.

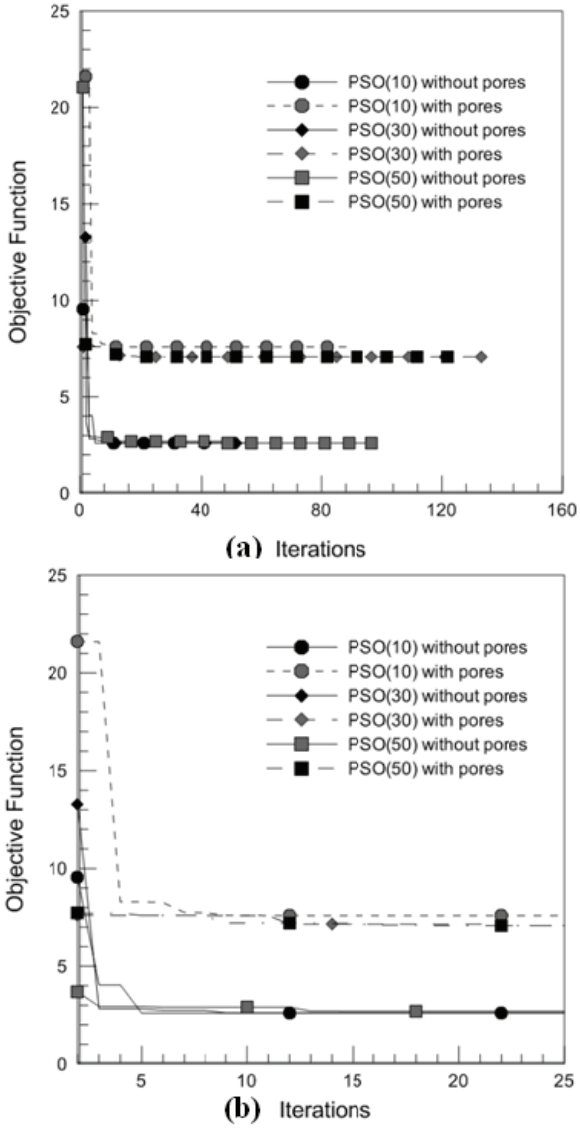

Figure 5. Effects of population size on PSO convergence (Ste = 0.58).

Table 4 shows results for estimated porosity performed with different levels of random noise introduced on the synthetic experimental data, considering 10 particles in the population. As expected, by increasing the noise level, the error

found in the estimated porosity is also increased. For 10% of random noise level, 15% of relative error is obtained for the estimated porosity. Nevertheless, by increasing the noise, the CPU time and the number of iterations to reach the convergence showed non-monotonic behaviors. This can be explained by the adopted stopping criterion. The noise hinders the convergence and establishes a limit for the minimization process, as seen in Figure 6. By increasing the noise, the value of this limit is also increased, thus reducing the number of required iterations for convergence. As expected, the noiseless case shows the best results for the parameter estimated, spending less time, since the solidification model was built for this case.

Table 3. Effect of the number of particles on the optimal solution (Ste = 0.58, ε = 0.7).

Number of particles	CPU time (s)	Objective function	Estimated (ε)	Iterations
10	12970.86	7.588358	0.711694	90
30	57537.69	7.076548	0.713076	134
50	87938.34	7.076548	0.713076	123

Table 4. Effect of random noise level on the estimated porosity (Ste = 0.58, ε = 0.7).

Noise level	CPU time (s)	Objective function	Estimated (ε)	Iterations
0.00	12970.86	7.588358	0.711694	90
0.01	18794.43	12.816717	0.697859	130
0.05	17872.41	49.404762	0.637428	124
0.10	14450.62	291.200131	0.605754	100

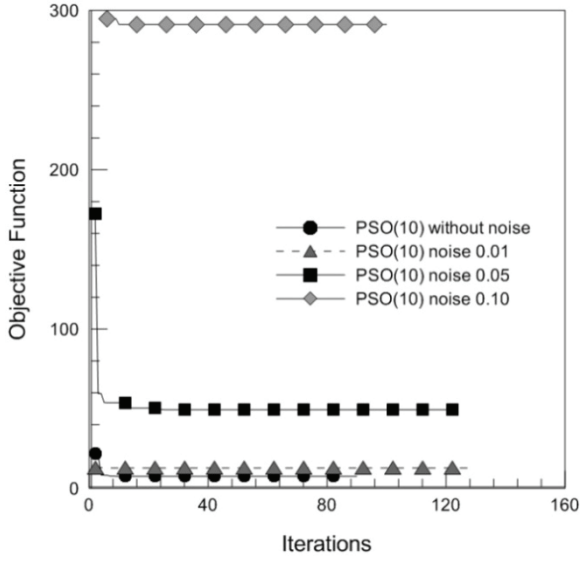

Figure 6. Effects of population size on PSO convergence for noise data (Ste = 0.58, ε = 0.7).

Conclusion

In this study, a mathematical model based on an effective heat capacity approach was proposed. The Finite Volume Method was employed to solve this model by using the explicit scheme and the central differences interpolation function.

The numerical solution was verified and reference results for solidification processes with and without pores were reproduced. The disagreements found between those solutions were due to differences in the models, since the model proposed in this study considers a finite domain and the reference results were obtained from models for semi-infinite domains.

The results showed that porosity reduces the solidification velocity, because it diminishes the effective diffusivity of the solid. Therefore, by increasing the porosity, total solidification time is also increased. Thus, measurements of the total time of solidification and the heat flux at the boundary wall can be used to predict the porosity formation.

The particle swarm optimization was employed in the inverse problem to estimate the porosity. The effects of the population size on PSO performance were analyzed, indicating that 10 particles were enough to execute the computations. The objective function was built, considering synthetic experimental data of the position of the solidification front, which were related to the heat flux at the boundary wall.

The results of the inverse problem were verified, estimating correctly the porosity parameter for noiseless synthetic experimental data. However, when noise was increased, the porosity estimation became less accurate.

This study focused on the prediction of the porosity formed during the solidification process of TNT. The provided information can be used for planning the process of fabrication of high-explosive ammunitions in order to avoid pores and voids inside the solidified explosive. Furthermore, this study has shown that the level of porosity can be estimated by using an inverse problem technique.

Acknowledgements

The authors acknowledge the support provided by Brazilian Army and CAPES.

References

Bauer, T. H. (1993). A general analytical approach toward the thermal conductivity of porous media. *International Journal of Heat and Mass Transfer, 36*(17), 4181-4191.

Chávez, C. E., Alonzo-Atienza, F., & Álvarez, D. (2013). Avoiding the inverse crime in the inverse problem of electrocardiography: estimating the shape and location of cardiac ischemia. *Computing in Cardiology, 40*(1), 687-690.

Colaço, M. J., Orlande, H. R. B., & Dulikravich, G. S. (2006). Inverse and optimization problems in heat transfer. *Journal of Brazilian Society of Mechanical Sciences and Engineering, 28*(1), 1-24.

Gibson, L., & Ashby, M. (1997). *Cellular solids: structure and properties*. Cambridge, MA: University Press.

Hu, H., & Argyropoulos, S. A. (1996). Mathematical modeling of solidification and melting: a review. *Journal of Heat Transfer, 4*(4), 371-396.

Humphreys, N. J., Mcbride, D., Shevchenko, D. M., Croft, T. N., Withey, P., Green, N. R., & Cross, M. (2013). Modelling and validation: Casting of Al and TiAl alloys in gravity and centrifugal casting processes. *Applied Mathematical Modelling, 37*(14-15), 7633-7643.

Iacono, C., Sluys, L., & Van Mier, J. G. M. (2011). Inverse procedure for parameters identification of continuum damage models. In M. J. Colaço, H. R. B. Orlande, & G. S. Dulikravich (Eds.), *Inverse problems design and optimization* (p. 223-229). Rio de Janeiro, RJ: E-papers.

Jaccoud, B. R., Caldeira, A. B., & Guedes, R. O. C. (2014). Efeitos da porosidade na transferência de calor durante o processo de solidificação do TNT. *Revista Militar de Ciência e Tecnologia, 31*(4), 1-13.

Kumar, A. S., & Rao, V. D. (2014). Modeling of cooling and solidification of TNT based cast high explosive charges. *Defence Science Journal, 64*(4), 339-343.

Machado, H. A., & Orlande, H. R. B. (1998). Inverse problem for estimating the heat flux to a non-newtonian fluid in a parallel plate channel. *Journal of the Mechanical Society of Mechanical Sciences, 20*(1), 51-61.

Maliska, C. (2004). *Transferência de calor e mecânica dos fluidos computacional* (2a ed.). Rio de Janeiro, RJ: LTC.

Mosaffa, A. H., Ferreira, C. A. I., Talati, F., & Rosen, M. A. (2013). Thermal performance of a multiple pcm thermal storage unit for free cooling. *Energy Conversion and Management, 67*(1), 1-7.

Ozisik, M. N., & Orlande, H. R. B. (2000). *Inverse heat transfer*. New York City, NY: Taylor & Francis.

Poirier, D., & Salcudean, M. (1998). On numerical methods used in mathematical modeling of phase change in liquid metals. *Journal of Heat Transfer, 110*(3), 562-570.

Stefan, J. (1891). Uber die theorie der eisbildung, inbesondere uber die eisbildung im polarmeer. *Annalen der Physik und Chemie, 42*(2), 269-86.

Sun, D., & Garimella, S. (2007). Numerical and experimental investigation of solidification shrinkage. *Numerical Heat Transfer, Part A: Applications, 52*(2), 145-162.

Tan, H., Li, C., & Li, Y. (2011). Simulation research on pcm freezing process to recover and store the cold energy of cryogenic gas. *International Journal of Thermal Sciences, 50*(11), 2220-2227.

Verma, S. P., & Gómez-Arias, E. (2013). Three-dimensional temperature field simulation of magma chamber in the Los Humeros geothermal field. *Applied Thermal Engineering, 52*(2), 512-515.

Wang, J., Carson, J., North, M., & Cleland, D. (2006). A new approach to modelling the effective thermal conductivity of heterogeneous materials. *International Journal of Heat and Mass Transfer, 49*(17-18), 3075-3083.

Yajun, W., Pengfei, F., Yongjun, G., Zhijun, L., & Yintao, W. (2013). Research on modeling of heat source for electron beam welding fusion-solidification zone. *Chinese Journal of Aeronautics, 26*(1), 217-223.

Zhang, B., Kim, T., & Lu, T. (2009). Analytical solution for solidification of close-celled metal foams. *International Journal of Heat and Mass Transfer, 52*(1-2), 133-141.

Zhang, Q., Hu, S., & Liang, H. (2013). Effect of pore in composition-B explosive on sensitivity under impact of drop weight. *Defence Science Journal, 63*(1), 108-113.

Received on May 30, 2015.
Accepted on October 8, 2015.